

PROCEEDINGS OF SPIE

SPIDigitalLibrary.org/conference-proceedings-of-spie

Dynamical anisotropy of the optical propagation paths

Tatiana I. Arsenyan, Maksim V. Pisklin, Natalia A. Suhareva, Aleksey M. Zotov

Tatiana I. Arsenyan, Maksim V. Pisklin, Natalia A. Suhareva, Aleksey M. Zotov, "Dynamical anisotropy of the optical propagation paths," Proc. SPIE 9680, 21st International Symposium Atmospheric and Ocean Optics: Atmospheric Physics, 96801Z (19 November 2015); doi: 10.1117/12.2205803

SPIE.

Event: XXI International Symposium Atmospheric and Ocean Optics. Atmospheric Physics, 2015, Tomsk, Russian Federation

Dynamical anisotropy of the optical propagation paths

Tatiana I. Arsenyan, Maksim V. Pisklin, Natalia A. Suhareva and Aleksey M. Zotov

Lomonosov Moscow State University, Leninskie Gory, Moscow, 119991, Russian Federation

ABSTRACT

Dynamics of laser beam intensity profile spatial modulations over a model tropospheric path with the controlled meteorological parameters was studied. Influence of the underlying surface temperature as well as the side wind load were considered. The increase of dynamic anisotropic disturbances saturation with the path length was observed. Spatio-temporal correlation characteristics of the directivity pattern in the signal beam registration plane were obtained. Proposed method of the experimental samples analysis on the base of chronogram with the following definition of the dynamic structure tensors array allows to estimate local and averaged projections of the flow velocities over the chosen spatio-temporal region and to restore their geometry in the zone of intersection with the signal beam. Additional characteristics suggested for the diagonalized local structure tensors such as local energy capacity and local structuredness are informative for the estimation of the inhomogeneities spatial dimensions, time of access through the section considered, the dynamics of energetic jets. The concepts of rotational and translational dynamic anisotropy are introduced to discriminate the types of the changes of the local ellipsoids axes orientation as well as their values. Rotational anisotropy shows itself in the changes of the local ellipsoids orientation, thus characterizing the illumination variation over the beam cross-section. Translational anisotropy describes the difference between the axes values for local ellipsoids.

Keywords: Free space optical channel, turbulence, tensor structure elements, dynamical anisotropy, rotational and translational anisotropy components

1. INTRODUCTION

Noise-proved coding of the signal optical beams on the base of structurally stable solutions and non uniform polarization state demands the investigation of the detailed dynamics of the beam profile variations. The attention in describing of these variations must be focused on the short-range modulations of the beam profile relating to diverse laminar and turbulent structures. One can characterize each of these structures by a positional parameter (region of initiation), two statistical ones (the probability of initiation and the lifetime) and two vector dynamic ones (angular moment flow and impulse flow).

This work considers the dynamic of the signal optical beam variation over the model path with strong convective flows due to vertical temperature gradient and horizontal wind load. Strict conditions of strong non-stationarity, non-equilibrium and inhomogeneity of the refractivity spatial variations demand new experimental approaches to investigations of the dynamics of the signal beam profile distortions and to selection of the controlled parameters. Processing algorithm for the experimental samples and its hardware implementation must be in agreement with characteristic quasi-stationary periods of the processes along the path.

2. SYNTHESIS OF THE CHRONOGRAM FOR THE RECORDING SESSION

The results were obtained using a model experimental path similar to the tropospheric one. It was equipped with a heating element in the bottom and the side nozzles to simulate the wind load. To change the path length the driving flat mirrors with variable tilt angles were used. The maximum path length in the model device was about 15 m. Strong fluctuations conditions were produced along the model path. To avoid uncontrollable temperature and aerodynamic effects the working zone was enclosed in the cylindrical tube of 0.25 m diameter

Further author information: (Send correspondence to Maksim V. Pisklin)
Maksim V. Pisklin: E-mail: maxim.pisklin@gmail.com, Telephone: +7 495 939 4601

with slot windows at the ends. The second harmonic solid state laser was used as a radiation source. It generated a Gaussian beam with a working diameter of 0.5 cm at a wavelength $\lambda = 0.48$ micrometers.¹

The dynamics of intensity distribution at the path output was recorded using a high-speed PULNiX-1300 camera. It allowed video recording of the process with the frame frequency of 400 Hz and higher without additional compression and filtration at a working field resolution of 320x240 points and 8-bit intensity coding. The duration of individual video sample was not less than 20s. Time sampling was equal to 2.5 ms, working frame was 320x240 pixel under the 8-bit digitization of the local intensity, thus being equivalent to 8000 frames for each sample.²

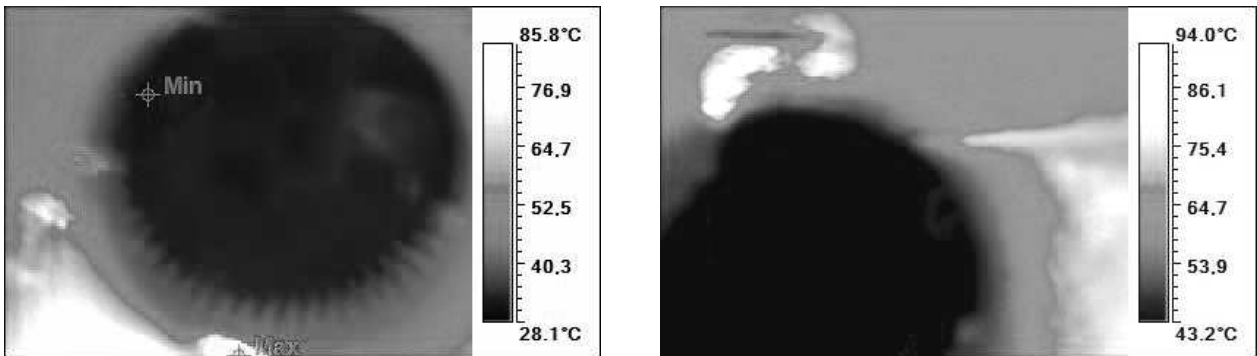


Figure 1. The examples of thermal flows in active zone of experimental path

Thermal non-equilibrium state of the medium along the beam propagation path is created by the lengthy heating element placed in the bottom of the bounding case. Its temperature can be regulated in the interval from the room temperatures up to 350°C. Under the conditions of dynamic equilibrium the temperature gradient averaged along the path can achieve the value of 2000 degrees per meter. The selected interval of temperature gradient values allows to investigate different types of laser beam distortions, - weak distortions, strong turbulence mode, as well as the coherent turbulence mode accompanied by Rayleigh-Bernard convective flows.³

Fig. 1 represents the typical dynamic profiles geometry of the temperature distribution in the near-surface protecting case of the model path. The registration was carried out using the thermal imager. Inhomogeneous structure of the underlying surface as well as the irregularity of its heating results in strong asymmetry of up-flows. They are intensified by thermodynamic nonstationarity of the gaseous medium. The dynamics of the temperature distribution in the path active zone substantially depends on the underlying surface temperature. Under low heating temperatures (less than 75°C) practically linear temperature decrease takes place in vertical to this surface direction. Temperature interval from 75°C to 200°C is characterized by generating of several large vertical and spiral flows having characteristic dimensions up to 0.2L. Here L is the case lateral dimension. Further increasing of the temperature leads to forming of the heat wall shell inside the case, thus essentially changing the temperature gradients geometry and the symmetry of the convective flows. In addition the character of flows becomes more complicated because of the flank wind load which transforms the temperature fields as well as the aerodynamic profiles.

Experimental study of a signal beam spatial profile was carried out. We analyzed the trajectories got under the process of tracing of the structural elements intensity distribution in the case of wide-aperture signal beam detection. For this purpose the laboratory model of optical path was build. Meteorological conditions along the path can be changed. This allowed to get different convective flows profiles including spiral ones and those referred to the conditions of coherent turbulence. Using of the tracing method permitted to create a macro frame completed during the real-time operation.

Initially got video sample was divided into sequence of frames. From each frame, the horizontal and vertical strips were cut out, their width being equal to 1 pixel. Consecutive merging of these strips allowed to get horizontal and vertical macro frames representing a couple of chronograms (Fig. 2).

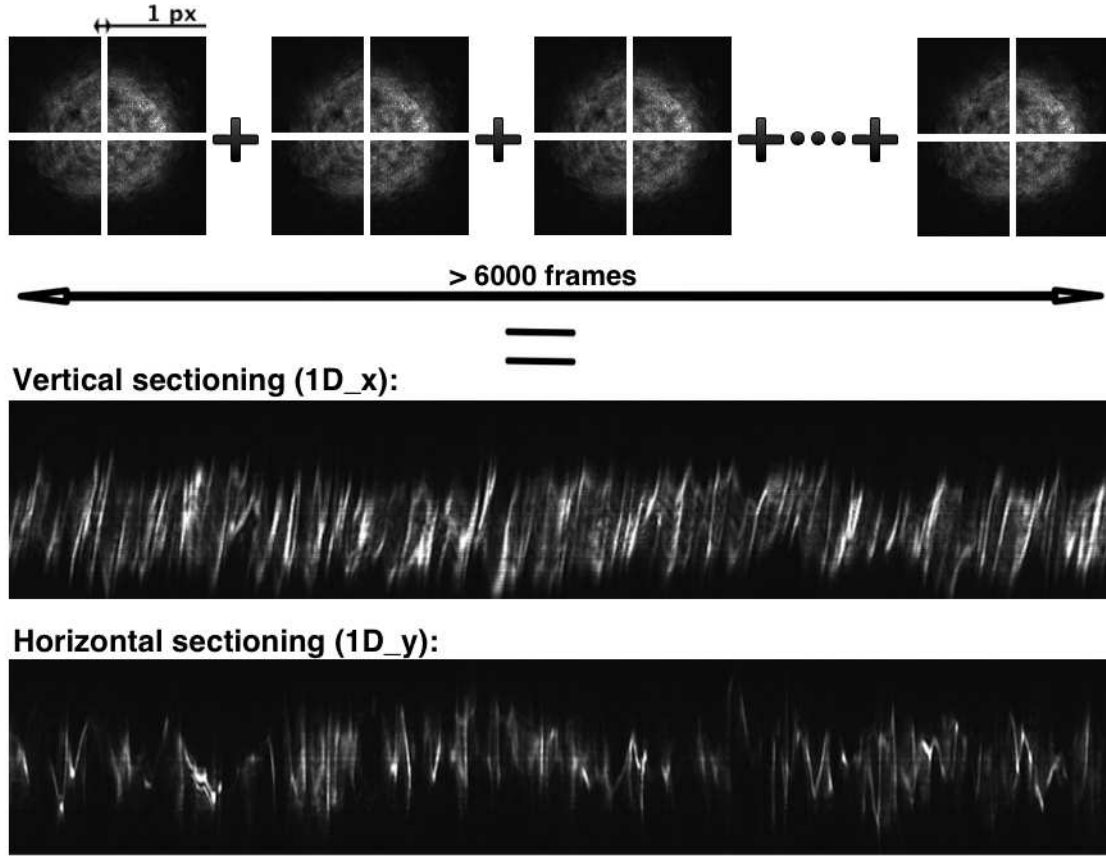


Figure 2. Generation of vertical and horizontal chronograms

3. TENSOR ANALYSIS OF THE ANISOTROPIC DISTORTIONS DYNAMICS

Let us define the local tensor of the dynamic system as follows⁴ :

$$\hat{J}(t, s) = \begin{bmatrix} J_{tt} & J_{st} \\ J_{ts} & J_{ss} \end{bmatrix} \quad (1)$$

The tensor structure elements associated with the chronogram point (s, t) one can get by the derivatives averaging for the corresponding coordinates over the chosen window:

$$J_{tt}(s, t) = \sum_{\tau}^T \sum_{\xi}^N w(s - \xi, t - \tau) \left(\frac{\partial I(\xi, \tau)}{\partial \tau} \right)^2, \quad (2)$$

$$J_{ss}(s, t) = \sum_{\tau}^T \sum_{\xi}^N w(s - \xi, t - \tau) \left(\frac{\partial I(\xi, \tau)}{\partial \xi} \right)^2, \quad (3)$$

$$J_{ts}(s, t) = J_{st}(s, t) = \sum_{\tau}^T \sum_{\xi}^N w(s - \xi, t - \tau) \left(\frac{\partial I(\xi, \tau)}{\partial \xi} \right) \left(\frac{\partial I(\xi, \tau)}{\partial \tau} \right), \quad (4)$$

here T - is the number of frames used for the chronogram synthesis, N - is the number of rows or columns (vertical or horizontal selection) of the initial image, $w(s, t)$ - normalized window weight function. In the following

calculations the Gaussian profile was used having 1pt variance in both directions. Diagonal and non-diagonal structure tensor elements created on the base of partial derivatives carry the information about the local dynamics of the light intensity level of the image elements. The dynamic structure tensors are defined at each point of the discrete image. Accordingly one gets 1440000 tensors of structure for the image size 240pt*6000pt.

Each tensor structure from the massive obtained can be brought to diagonal form by the rotation of the supporting coordinates system through the appropriate angle. Such an angle and the pair of diagonal elements is introduced for every pixel of the discrete image. The meaning of the rotation angle needed for local tensor diagonalization one gets using the following condition^{5,6} :

$$\begin{bmatrix} J_1 & 0 \\ 0 & J_2 \end{bmatrix} = \begin{bmatrix} \cos \theta & \sin \theta \\ -\sin \theta & \cos \theta \end{bmatrix} \begin{bmatrix} J_{tt} & J_{st} \\ J_{ts} & J_{ss} \end{bmatrix} \begin{bmatrix} \cos \theta & -\sin \theta \\ \sin \theta & \cos \theta \end{bmatrix} \quad (5)$$

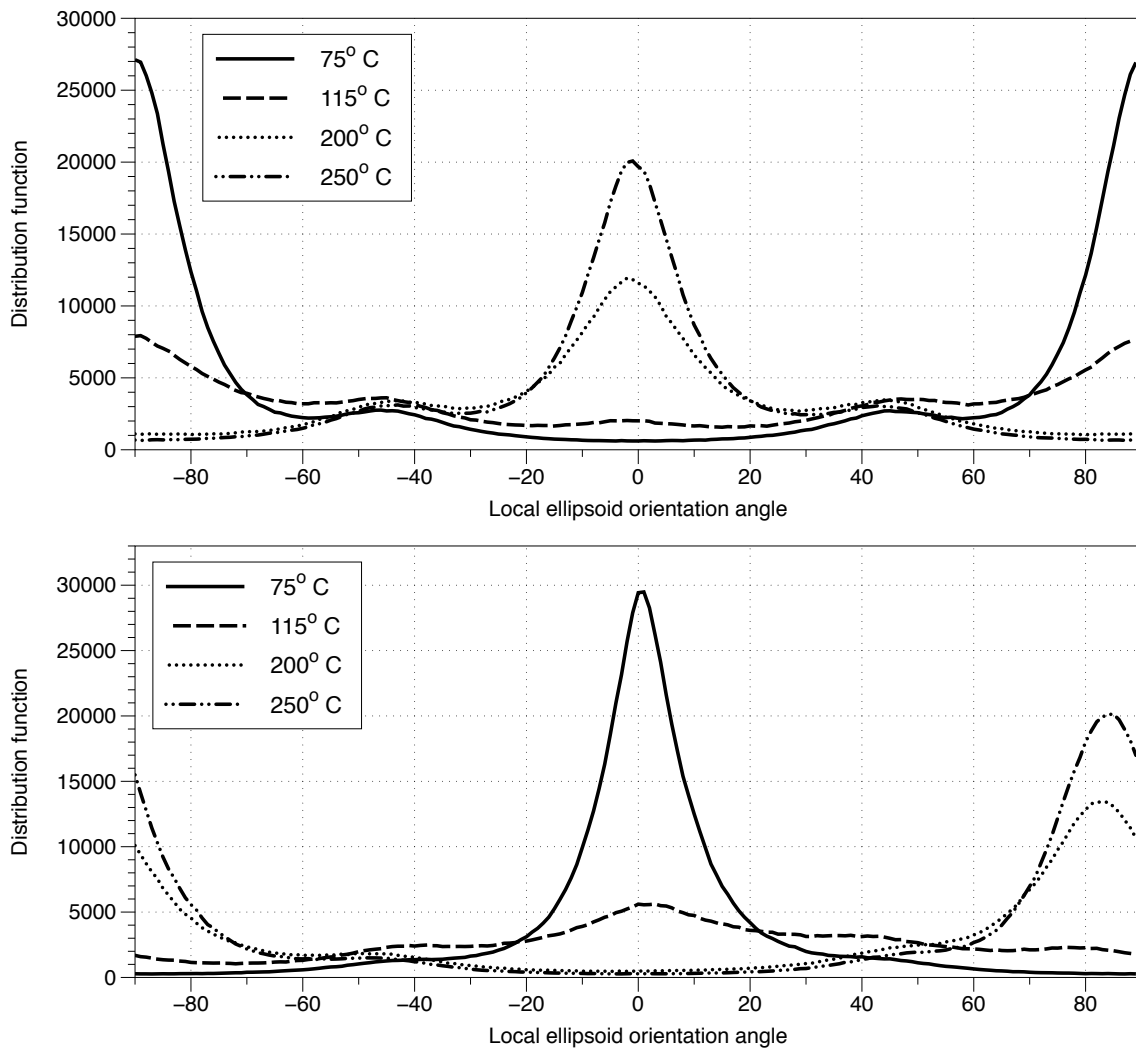


Figure 3. Local orientation statistics (upper - horizontal, bottom - vertical). Wind velocity is 3 m/s, path length is 9 m

Application of the nullification condition for the non-diagonal elements as a result of double matrix multiplication in the right sight of equation (5) allows to obtain the value of the rotation angle needed or the local ellipsoid orientation⁷ :

$$(J_{ss} - J_{tt}) \sin 2\theta + 2J_{st} \cos 2\theta = 0, \quad (6)$$

$$\theta(s, t) = \frac{1}{2} \arctan \left(\frac{2J_{st}(s, t)}{J_{tt}(s, t) - J_{ss}(s, t)} \right) \quad (7)$$

Rough estimation of the dynamic orientation characteristics one can carry out on the base of distribution function profile for the local ellipsoids axes orientations. Fig. 3 represents the typical distribution function profiles for the angles of local ellipsoids orientations obtained for horizontal and vertical chronograms. The main difference of these distributions consists in the violation of the vertical chronogram symmetry relative to zero value of the rotation angle. That can account for the preferred orientation of the supporting coordinates system for the tensor structure stimulated by the air masses motions.

Besides the orientation and axes values of local ellipsoids, several additional parameters are used as a rule. One of them is equivalent to "visibility" of the differential image (J_1 and J_2 are upbuilt on the base of differentials) and can be named as a degree of dynamic structural properties:

$$C(s, t) = \frac{(J_{tt}(s, t) - J_{ss}(s, t))^2 + 4J_{ts}(s, t)J_{st}(s, t)}{(J_{tt}(s, t) + J_{ss}(s, t))^2} = \left(\frac{J_1(s, t) - J_2(s, t)}{J_1(s, t) + J_2(s, t)} \right)^2 \quad (8)$$

The time-spatial distributions of this value typical for chronograms studied are presented in Fig. 4. The brightness of the image pixel is proportional to the value of the structural properties, which in its turn possesses the value inside the interval $[0, 1]$. Zero value of the structural properties function corresponds to uniform illumination of all the chronogram elements. The structural properties function are equal to 1 when the spatial inhomogeneity is fixed in the quiescent state or in the state of movement.

It is interesting to analyze one more characteristics - the so called "energetic capacity". This value is defined on the base of second powers of the temporal and spatial variation of the illumination level. In this occasion one can interpret the time derivative $\frac{\partial I(s, t)}{\partial t}$ as the velocity of the local illumination changes, and the coordinate derivative $\frac{\partial I(s, t)}{\partial s}$ can be treated as the spatial deformation of the local illumination:

$$E(s, t) = J_{ss}(s, t) + J_{tt}(s, t) \sim \left(\frac{\partial I(t, s)}{\partial t} \right)^2 + \left(\frac{\partial I(t, s)}{\partial s} \right)^2 \sim U(s, t) + T(s, t) \quad (9)$$

The coordinates transformation (5) conducted for the diagonalization of the tensor structure preserves the spur of matrix.⁸ That means the validity of the assumption

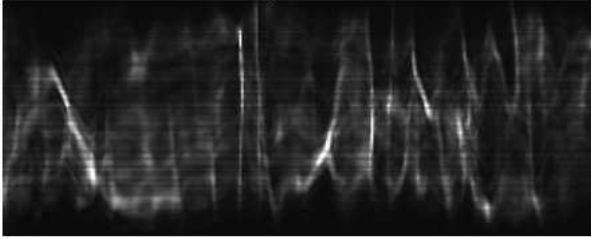
$$J_1(s, t) + J_2(s, t) = J_{ss}(s, t) + J_{tt}(s, t), \quad (10)$$

which is equivalent to the conservation of energetic capacity under the conditions of coordinate system rotation. But several components of the energetic capacity may change their values.⁹ The rule for such changes can be written as follows:

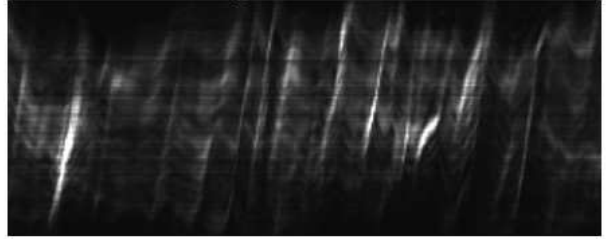
$$J_1(s, t) - J_2(s, t) = (J_{ss}(s, t) - J_{tt}(s, t)) \cos 2\theta + 2J_{st}(s, t) \sin 2\theta \quad (11)$$

Bottom picture of the Fig. 4 represents space-time distribution of the energetic capacity. Well-marked space-time maxima are informative for the analysis of the mechanisms of beam distortions. All the differential characteristics presented were obtained using image processing application ImageJ¹⁰ and plugin OrientationJ,¹¹ based on processing of the local tensors characteristics of the image structure.

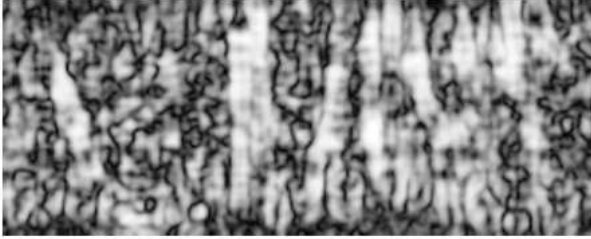
Horizontal sectioning:



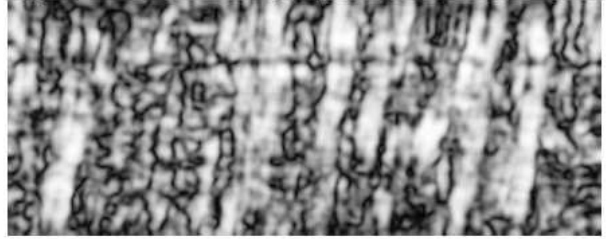
Vertical sectioning:



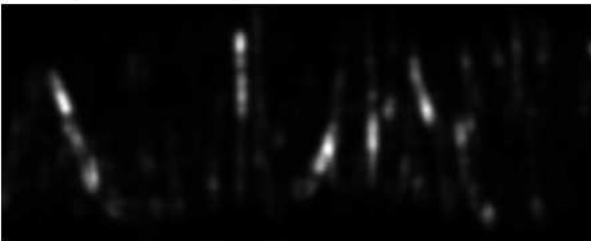
Dynamic structural properties:



Dynamic structural properties:



Energetic capacity:



Energetic capacity:

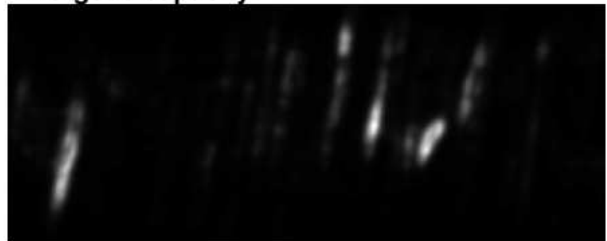


Figure 4. Space-temporal structural properties (middle), energetic capacity (bottom) of initial chronograms for vertical and horizontal sections (upper)

Dynamic anisotropy manifests itself through a local non-equivalence of the drift angle and redistribution of the illumination levels of the image. In some cases the angle of local ellipsoid orientation allows to define the values of drift velocity. Let us consider a chronogram, corresponding to the sequence of the level of illumination distributions described as a drift with the velocity u along the s - coordinate without the changing of the common intensity profile:

$$I(s, t) = I(s - ut), \quad (12)$$

Fulfilling the demanded time and coordinate differentiations one obtains for the local ellipsoids orientation angles:

$$\theta(s, t) = -\tan \left(\frac{1}{2} \arctan \frac{-2u \left(\frac{\partial I(s, t)}{\partial s} \right)^2}{\left(\frac{\partial I(s, t)}{\partial s} \right)^2 - u^2 \left(\frac{\partial I(s, t)}{\partial s} \right)^2} \right) = u. \quad (13)$$

If besides the beam drift on the surface the redistribution of the illumination level takes place -

$$I(s, t) = I(s - ut; t) \quad (14)$$

the relation between the drift velocity and the angles of local ellipsoids orientation is not so obvious:

$$\theta(s, t) = \tan \left(\frac{1}{2} \arctan \frac{u \left(\frac{\partial I(s, t)}{\partial s} \right)^2 - \left(\frac{\partial I(s, t)}{\partial s} \right) \left(\frac{\partial I(s, t)}{\partial t} \right)}{(1 - u^2) \left(\frac{\partial I(s, t)}{\partial s} \right)^2 + 2u \left(\frac{\partial I(s, t)}{\partial s} \right) \left(\frac{\partial I(s, t)}{\partial t} \right) - \left(\frac{\partial I(s, t)}{\partial t} \right)^2} \right). \quad (15)$$

Disalignment of the changes of the sections chronogram along spatial and temporal coordinates does not allow simple interpretation of the local rotation angle $\theta(s, t)$ as a measure of drift velocity. Nevertheless the possibility to define the chronogram averaged overall velocity of the illumination profile drift as well as its variance taking into account the variance of the beam intensity profile, persists.

4. LOCAL ORIENTATIONS STATISTICS

Multimodal profile of the distribution function, - the presence of the several maxima in the probability distribution, - allows to analyze the anisotropic properties of the illumination levels local changes under the conditions of changing of the model path meteoroparameters at the stages of separate peaks as well as for the distribution function moments in tote.

Let us consider the influence of the underlying surface temperature on the location of the distribution function main maxima in the vertical chronogram obtained for the different model path lengths (6, 9, 12 and 15 m), the underlying surface temperature being equal to 335°C and in the absence of the wind load (Fig. 5).

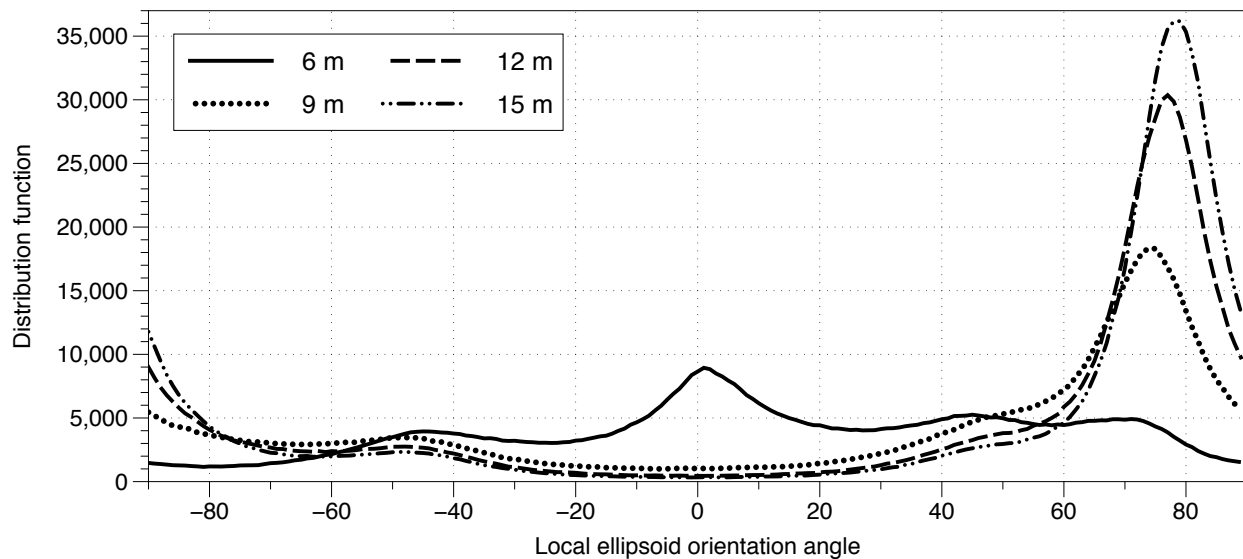


Figure 5. The distribution function for angles of local ellipsoid orientation in the case of vertical chronogram

Two maxima locations of the distribution function are allowed. One of them corresponds to undisturbed beam passed the path in the absence of vertical disturbances and characterized by local ellipsoid deviation angle equal to zero (horizontal line on chronogram). The other maximum is predefined by the spiral flow. With the path length increasing the variance of the local maximum displaced from the center persists. It can be accounted for the constant temperature of the underlying surface. The maximum location is practically constant within the inaccuracy range of the measurements conducted as far as under the given thermal non-equilibrium state and

the fixed geometry, the spiral flow geometry appears to be determined and does not depend on effective path length.

The first moment of the distribution function gives the information about the flank wind loading. In the experiment, the wind velocity varied in the range from 0 m/s to 8 m/s. The experimental results are presented in Fig. 6. The average angle value for horizontal chronogram is within the range of instrumental and processing errors and manifests least noticeable difference from zero for any values of temperature and wind loading.

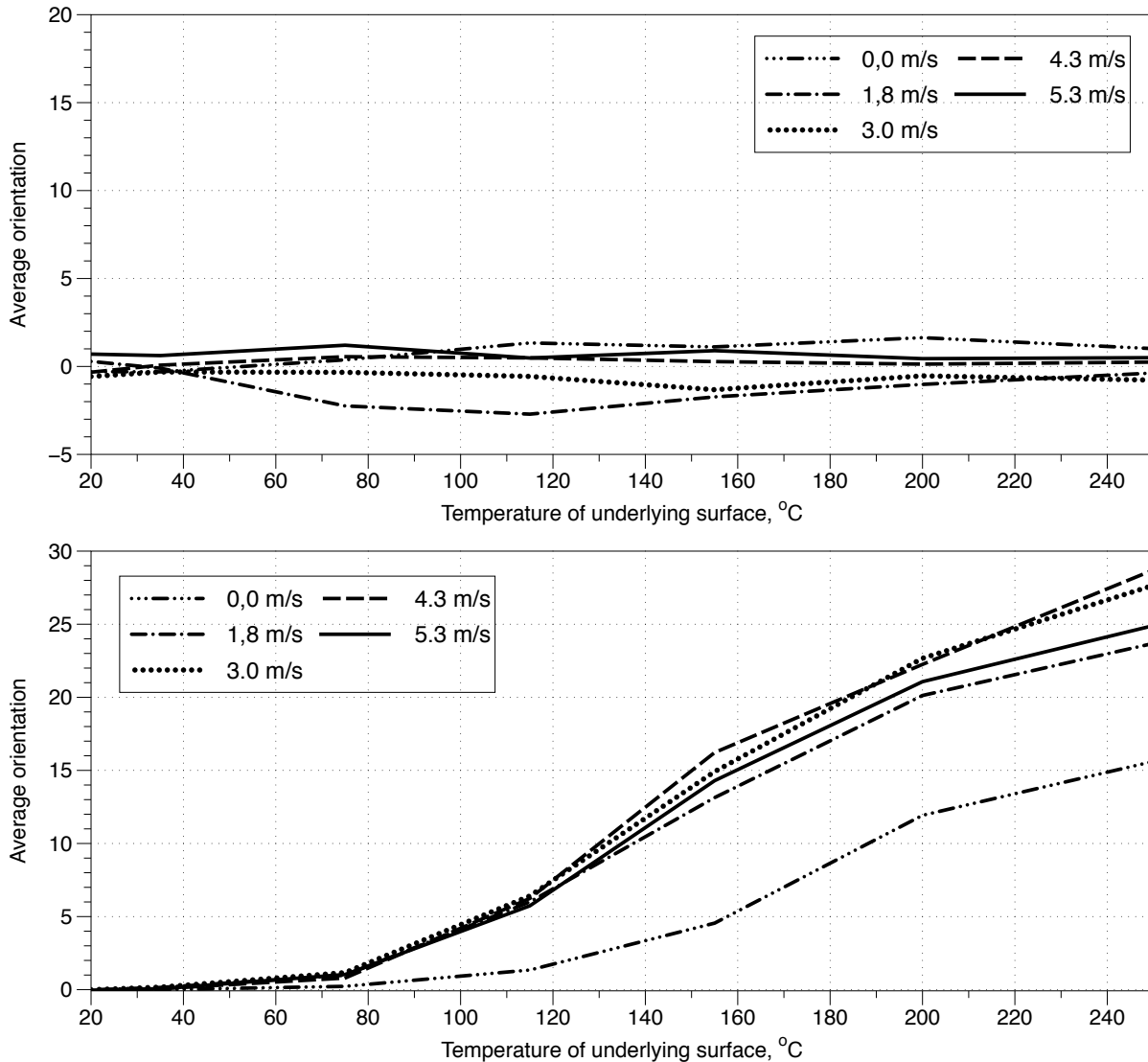


Figure 6. The average value of the chronogram orientation angle

The different situation is observed in the vertical chronogram. Under the absence of the wind loading the calculated average angle of rotation monotonically increases beginning from the threshold temperature (75°C) which permits the coherent turbulence appearance.³ One can notice several points of sharp bend of the average rotation angle, 120°C, 160°C, 200°C, - corresponding to involvement of additional vertical components. The wind loading practically spreads the vertical flow over the path volume thus increasing the interaction cross-section with the propagating beam. It is necessary to point out that within the velocity range from 1.8 m/s to 4.3 m/s the flank wind loading does not distort the existing vortical flow but adds to it an additional horizontal component not violating rotational or vertical components of aerodynamic flows. When the flank wind velocity

exceeds the value of about 4.3 m/s the flows begin to collapse. This manifests itself in the decreasing of the distribution function first moment.

5. CONCLUSIONS

Dynamic anisotropy manifests itself under the conditions of the paths having strong inhomogeneities of the thermal distributions which give rise to the states of coherent turbulence and spiral flows. The proposed method of the experimental samples analysis on the base of $1D_x$ and $1D_y$ chronogram and the following definition of the dynamic structure tensors array allows to estimate local and averaged projections of the flow velocities over the chosen spatio-temporal region and to restore their geometry in the zone of intersection with the signal beam.

The additional characteristics created for the diagonalized local structure tensors such as local energy capacity and local structuredness are informative for the estimation of the inhomogeneities spatial dimensions, time of access through the section considered, the dynamics of energetic jets. In the experimental model studied, only one mode of spiral flows is realized. Accordingly to this the characteristic spectrum of the local ellipsoids rotation angles persists. For the real paths, these spectra will be different. They will contain the information about the non-equilibrium statistics and non-stationary dynamics of the flows.

It is helpful to use the concepts of rotational and translational dynamic anisotropy to discriminate the types of the changes of the local ellipsoids axes orientation as well as their values. Rotational anisotropy shows itself in the changes of the local ellipsoids orientation, characterizing the illumination variation over the beam section. Translational anisotropy describes the difference between the axes values for local ellipsoids.

ACKNOWLEDGMENTS

The work was carried out under the financial support of RFBR (grant 14-02-00461).

REFERENCES

- [1] Arsenyan, T. I., Suhareva, N. A., and Sukhorukov, A. P., "Turbulence-induced laser-beam distortions in phase space," *Moscow University Physics Bulletin* **69**(1), 55–60 (2014).
- [2] Arsenyan, T. I., Grebennikov, D. J., Suhareva, N. A., and Sukhorukov, A. P., "Reconstruction of phase trajectories of a laser beam propagated through a turbulent medium," *Atmospheric and Oceanic Optics* **27**(3), 205–210 (2014).
- [3] Getling, A. V., [*Rayleigh-Benard Convection: Structures and Dynamics*], Advanced Series in Nonlinear Dynamics (Book 11), World Scientific Pub Co Inc (1997).
- [4] Jahne, B., [*Spatio-temporal image processing: theory and scientific applications.*], Springer, Berlin (1993).
- [5] Unser, M., Aldroubi, A., and Eden, M., "B-spline signal processing: Part i - theory," *IEEE Transactions on Signal Processing* **41**(2), 821–833 (1993).
- [6] Bigun, J., Bigun, T., and Nilsson, K., "Recognition by symmetry derivatives and the generalized structure tensor," *Pattern Analysis and Machine Intelligence, IEEE Transactions on* **26**(12), 1590 – 1605 (2004).
- [7] Aubert, G. and Kornprobst, P., [*Mathematical problems in image processing: partial differential equations and the calculus of variations*], Springer, New York (2006).
- [8] Laidlaw, D. and Weickert, J., eds., [*Visualization and processing of tensor fields*], Springer, Berlin (2009).
- [9] Laidlaw, D. and Vilanova, A., eds., [*New developments in the visualization and processing of tensor fields*], Springer, Berlin (2012).
- [10] "Imagej - java image processing program, <http://imagej.nih.gov/ij/>."
- [11] "Imagej's plugin for directional analysis in images, <http://bigwww.epfl.ch/demo/orientation/>."